J. KSIAM Vol.12, No.1, 41–53, 2008

A NOTE ON PROLATE SPHEROIDAL WAVE FUNCTIONS AND PROLATE FUNCTION BASED NUMERICAL INVERSION METHODS

EUNJOO KIM AND JUNE-YUB LEE†

DEPT. OF MATH. AND INST. MATH. SCI., EWHA WOMANS UNIVERSITY, SEOUL 120-750, SOUTH KOREA
E-mail address: kej@math.ewha.ac.kr, jyllee@ewha.ac.kr

ABSTRACT. Polynomials are one of most important and widely used numerical tools in dealing with a smooth function on a bounded domain and trigonometric functions work for smooth periodic functions. However, they are not the best choice if a function has a bounded support in space and in frequency domain. The Prolate Spheroidal wave function (PSWF) of order zero has been known as a best candidate as a basis for band-limited functions.

In this paper, we review some basic properties of PSWFs defined as eigenfunctions of bounded Fourier transformation. We also propose numerical inversion schemes based on PSWF and present some numerical examples to show their feasibilities as signal processing tools.

1. INTRODUCTION

Polynomial is a good choice as a basis for smooth functions on bounded domain and trigonometric functions are more often used in signal processing purpose where signal is assume to be either periodic or measurable in infinite time. It is a classical question how to find a best basis function for (or simply to represent) a signal in infinite time domain from finite measurements under assumption that energy of the signal is bounded in frequency space.

The prolate spheroidal wave functions of order zero defined as eigenfunctions of bounded Fourier transformation, which will be referred as prolate functions in this paper, form a basis for band-limited functions. The prolate function has been thoroughly studied by D. Slepian and many other researchers [6, 7, 8, 9, 10, 11] in 1950-1970s to understand mathematical properties of band-limited functions. It has been widely referred in engineering community [2, 3] for more than 30 years, however, it was not commonly used as a numerical tool until recently due to its numerical instabilities. V. Rokhlin and his colleagues have developed numerically stable algorithms for PSWF evaluation, quadrature, and interpolation [12, 13]. In section 2. Mathematical Preliminaries, we basically follow the paper by H. Xiao, V. Rokhlin, and N. Yarvin in 2001 [12] and add mathematical details for better understanding of the basic properties of the prolate functions.

2000 *Mathematics Subject Classification.* 65R10, 33E10, 65R99.

Key words and phrases. Fourier Transformation, Sinc Operator, Band-limited Function, Signal Processing.

This work was supported by the Korea Research Foundation under grant no. KRF-2007-C00030.

† Corresponding author.

In section 3, we present two numerical inversion schemes to get the best matching function from given Fourier coefficients at a finite set of points in frequency domain. The first method is based on prolate interpolation of given signal and the second method is derived from a Lagrangian multiplier method. Some numerical examples are given in section 4 along with concluding remarks.

2. MATHEMATICAL PRELIMINARIES

2.1. **Bounded Fourier operator and Prolate Functions.** For positive real c, let F_c be the operator $L^2[-1,1] \to L^2[-1,1]$ defined by

$$F_c(\phi)(x) := \int_{-1}^{1} e^{icxt}\phi(t)\ dt. \tag{1}$$

It is clear that F_c is a compact linear operator since F_c is a bounded integral operator with L_2-integrable kernel.

Proposition 2.1. *For positive real c, the eigenvalues λ_m of F_c and the corresponding eigenfunctions ψ_m,*

$$F_c(\psi_m)(x) = \int_{-1}^{1} e^{icxt}\psi_m(t)\ dt = \lambda_m\psi_m(x) \tag{2}$$

can be chose as the following:

- *The eigenfunctions are real, orthonormal and complete in $L^2[-1,1]$.*
- *All eigenvalues are non-zero and either real or pure imaginary.*
- *The eigenfunctions corresponding to real eigenvalues are even and those to imaginary eigenvalues are odd.*

Proof. From the symmetry of e^{icst} on $[-1,1]$, it follows that if $\phi(x)$ is a solution of $\lambda\phi(x) = \int_{-1}^{1} e^{icxt}\phi(t)dt$, so are $\phi(-x)$ and $\phi(x) \pm \phi(-x)$. The eigenfunctions can be chosen to be either even or odd functions of x. The complex conjugate of equation is

$$\bar{\lambda}\bar{\phi}(x) = \int_{-1}^{1} e^{-icxt}\bar{\phi}(t)dt.$$

Multiplying above by $\phi(x)$ or $\bar{\phi}(x)$ and integrating, we get

$$(\lambda \pm \bar{\lambda}) \int_{-1}^{1} \phi(x)\bar{\phi}(x)dx = \int_{-1}^{1} dx \int_{-1}^{1} dt e^{icxt}\bar{\phi}(x)(\phi(t) \pm \phi(-t)).$$

If ϕ is even, by choosing the negative sign in this equation, one obtains $\lambda - \bar{\lambda} = 0$. If ϕ is odd, by choosing the plus sign, one finds $\lambda + \bar{\lambda} = 0$. The eigenvalues associated with even eigenfunctions are real. Those associated with odd eigenfunctions are pure imaginary.

It follows that eigenvalue-eigenfunction problem is equivalent to the pair of equations

$$\beta_e\phi_e(x) = \int_{-1}^{1} \cos(cxt)\ \phi_e(t)dt \tag{3}$$

and

$$\beta_o \phi_o(x) = \int_{-1}^{1} \sin(cxt)\, \phi_o(t) dt \tag{4}$$

in which β_e and β_o are real and non-negative. We observe that the eigenfunctions of (3) must be even and that $\beta_e = 0$ cannot be an eigenvalue of this equation. It follows that the eigenfunctions of (3) are complete in the class of even functions in $L^2([-1,1])$. Also we can derive similar arguments about (4). □

Definition 2.2. *A sequence of functions $\{\phi_1, \cdots, \phi_n\}$ will be referred to as a Chebyshev sequence on the interval [a,b] if each of them is continuous and the determinant*

$$\Delta \begin{pmatrix} \phi_1 & \cdots & \phi_n \\ x_1 & \cdots & x_n \end{pmatrix} := \begin{vmatrix} \phi_1(x_1) & \cdots & \phi_1(x_n) \\ \vdots & \ddots & \vdots \\ \phi_n(x_1) & \cdots & \phi_n(x_n) \end{vmatrix} \tag{5}$$

is nonzero for any sequence of points $x_1, \cdots, x_n$ such that $a \le x_1 < x_2 \cdots < x_n \le b$.

An alternative definition of a Chebyshev sequence is that any of linear combination of the functions with nonzero coefficients must have less than n-zeros.

Lemma 2.3. *Let $\{\phi_0, \phi_1, \cdots, \phi_m\}$ be a Chebyshev sequence. Then m-th function $\phi_m(x)$ in the sequence has exactly m-zeros if $\{\phi_0, \phi_1, \cdots, \phi_m\}$ is an orthogonal system.*

Proof. Let p be the number of zeros of $\phi_m(x)$ and $\{\xi_1, \cdots, \xi_p\}$ be the corresponding zeros. Consider an auxiliary function $\chi(x)$ defined as

$$\chi(x) := \Delta \begin{pmatrix} \phi_0 & \cdots & \phi_{p-1} & \phi_p \\ \xi_1 & \cdots & \xi_p & x \end{pmatrix}. \tag{6}$$

$\chi(x)$ has p-zeros at the exactly same locations as $\phi_m(x)$ since $\{\phi_0, \phi_1, \cdots, \phi_p\}$ is a Chebyshev sequence and the determinant is zero if and only if x coincides with one of $\{\xi_1, \cdots, \xi_p\}$. The inner product (χ, ϕ_m) on $[a, b]$ is not zero since two functions have the same zeros.

On the other hand, the orthogonality of $\{\phi_0, \cdots, \phi_p\}$ implies that

$$(\chi, \phi_m) = \int_a^b \begin{vmatrix} \phi_0(\xi_1) & \cdots & \phi_0(x) \\ \vdots & \ddots & \vdots \\ \phi_p(\xi_1) & \cdots & \phi_p(x) \end{vmatrix} \phi_m(x)\, dx = \begin{vmatrix} \phi_0(\xi_1) & \cdots & (\phi_0, \phi_m) \\ \vdots & \ddots & \vdots \\ \phi_p(\xi_1) & \cdots & (\phi_p, \phi_m) \end{vmatrix}$$

can be non-zero only when $p \ge m$. Therefore the number of zeros p must be exactly m since $\phi_m(x)$ can have at most m-zeros by the definition of Chebyshev sequence. □

Figure 1 shows the Prolate functions $\psi_m(x)$ for various $c = 1, 20, 50$ and the corresponding eigenvalues in decreasing order $|\lambda_m| \ge |\lambda_{m+1}|$. The m-th eigenfunction $\psi_m(x)$ has exactly m zeros on $[-1, 1]$ as shown in the figure (indeed, they form a Chebyshev sequence [1, 12]) and the (effective) support of $\psi_m(x)$ becomes narrower as c increases. It is also worth to remark that all eigenvalues are simple and even(odd) numbered eigenvalues are real(pure imaginary), more precisely $\lambda_m = i^m |\lambda_m|$ (See [12]). The solid lines in the right figure shows magnitude of

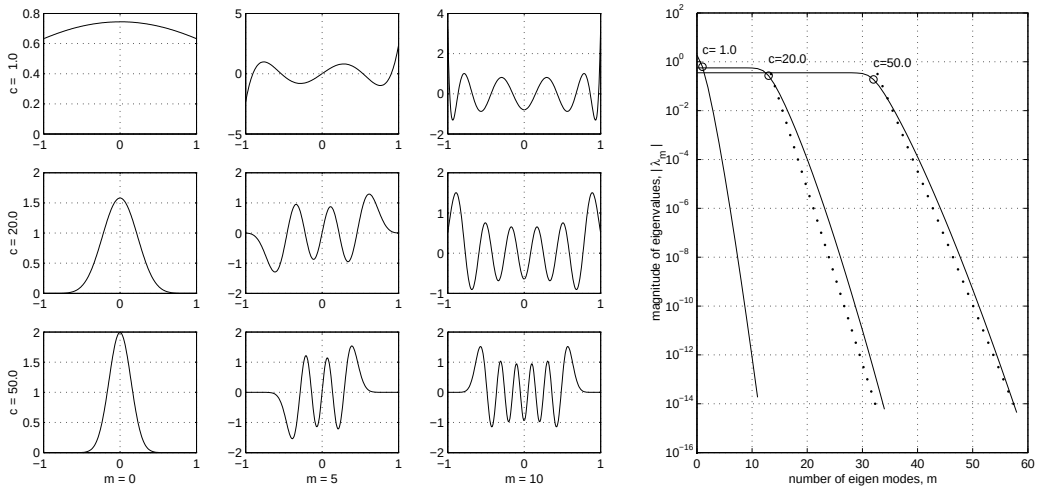

FIGURE 1. The 9 plots in the left show the prolate functions, $\psi_0, \psi_5, \psi_{10}$ for $c = 1, 20, 50$. Solid lines in the right figure draw the eigenvalues of F_c and dotted lines show the number of eigenvalues greater than ϵ, $N(c, \epsilon)$.

eigenvalues as a function of m for various c and number of eigenvalues whose absolute values are greater than ϵ is roughly $N(c, \epsilon) = \frac{2c}{\pi} + \frac{2}{\pi^2}\log(c)\log(\epsilon^{-1})$ for $1 \ll c \ll \epsilon^{-1}$, which plotted using dotted lines. (See [5] and Theorem 2.5 in [12]).

2.2. **Bounded Sinc-Operator.** We define a self-adjoint operator $Q_c : L^2[-1,1] \to L^2[-1,1]$ by the formula

$$Q_c(\phi)(x) := \frac{1}{\pi}\int_{-1}^{1} \frac{sin(c\cdot(x-t))}{x-t}\phi(t)\, dt. \tag{7}$$

then simple calculation shows

$$Q_c = \frac{c}{2\pi} F_c^* \cdot F_c \tag{8}$$

and Q_c has the same eigenfunctions $\psi_m(x)$ as F_c with the corresponding eigenvalue μ_m,

$$Q_c(\psi_m)(x) = \mu_m \psi_m(x) \ \text{ where } \ \mu_m = \frac{c}{2\pi}\cdot|\lambda_m|^2 . \tag{9}$$

Lemma 2.4. *For $x, t \in [-1,1]$, we have*

$$e^{icxt} = \sum_{j=0}^{\infty} \lambda_j \psi_j(x)\psi_j(t), \tag{10}$$

$$\frac{\sin c(x-u)}{x-u} = \frac{c}{2}\sum_{j=0}^{\infty} |\lambda_j|^2 \psi_j(x)\psi_j(u), \tag{11}$$

and

$$\sum_{j=0}^{\infty} |\lambda_j|^2 = 4, \quad \sum_{j=0}^{\infty} \mu_j = \frac{2c}{\pi}. \tag{12}$$

Proof. Since $\{\psi_i\}$ constitute a complete orthonormal basis in $L^2[-1,1]$, we have

$$e^{icxt} = \sum_{j=0}^{\infty} \left(\int_{-1}^{1} e^{icx\tau} \psi_j(\tau) d\tau \right) \psi_j(t), \quad \text{for all } x, t \in [-1,1]$$

and (10) is derived. Multiplying (10) by e^{-icut} and integrating with respect to t converts it into

$$\frac{\sin c(x-u)}{x-u} = \frac{c}{2} \sum_{j=0}^{\infty} |\lambda_j|^2 \psi_j(x) \psi_j(u).$$

Taking the square norm of (10) and integrating with respect to x and t yields the formula (12). □

2.3. **Extension of $\psi_m(x)$ into $L^2(-\infty,\infty)$.** We extend the eigenfunction $\psi_m(x)$ of F_c defined in (2) for $x \in (-\infty,\infty)$ as the following. For $x \in [-1,1]$,

$$\psi_m(x+n) := \frac{1}{\lambda_m} \int_{-1}^{1} e^{ic(x+n)t} \psi_m(t) dt. \tag{13}$$

Figure 2 shows the extended prolate function for $x > 0$ and $\psi_m(x)$ has even or odd symmetry depending on parity of m. $\psi_m(x)$ has always m-zeros and almost compactly supported on $[-1,1]$ if $m < \frac{2c}{\pi}$. $\psi_m(x)$ has m-zeros on $[-1,1]$ and small wiggling tails on $x > 1$ if $m \approx \frac{2c}{\pi}$, for examples, $m = 5$ and $c = 10$ or $m = 10$ and $c = 20$. $\psi_m(x)$ on $[-1,1]$ is exponentially small compared to the value on $x > 1$ when $m \gg \frac{2c}{\pi}$.

We also extend the bounded sinc operator $Q_c(\phi)(x) = \frac{1}{\pi} \int_{-1}^{1} \frac{\sin(c\cdot(x-t))}{x-t} \phi(t)\ dt$ defined in (7) for $x \in (-\infty,\infty)$ by replacing $x \in [-1,1]$ with $x+n$.

Lemma 2.5. *The extended prolate functions $\psi_m(x)$ defined in (13) also satisfy the following equation for the extended sinc-operator $Q_c : L^2[-1,1] \to L^2(-\infty,\infty)$,*

$$Q_c(\psi_m)(x+n) = \mu_m\, \psi_m(x+n). \tag{14}$$

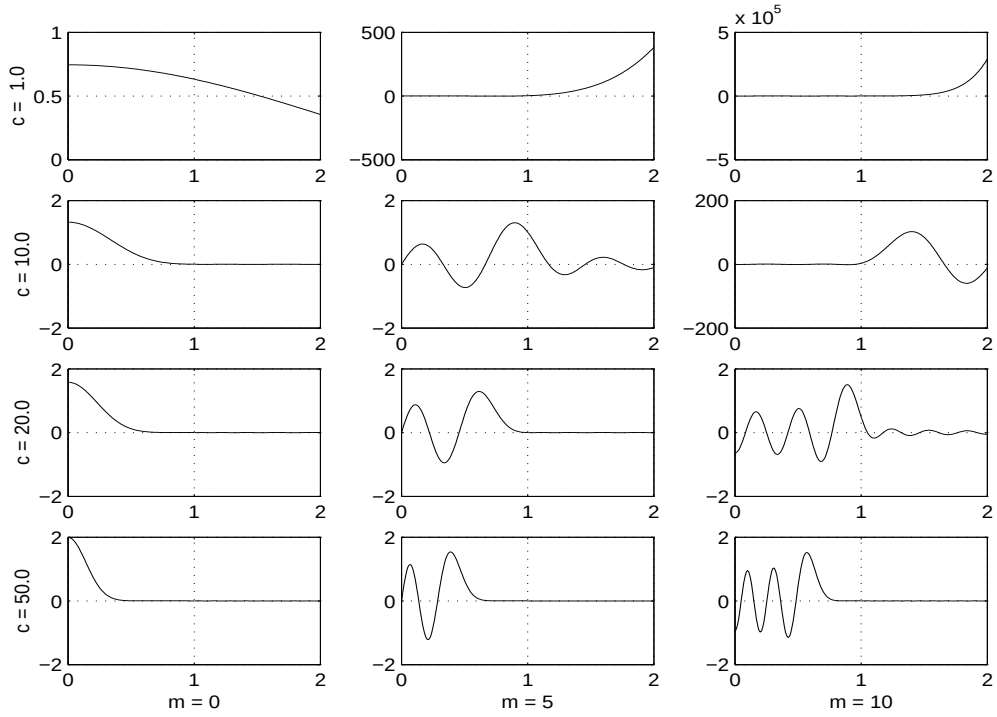

FIGURE 2. The extended prolate functions, $\psi_0, \psi_5, \psi_{10}$ for $c = 1, 10, 20, 50$.

Proof. A simple computation of $Q_c(\psi_m)(x+n)$ using the definition of Q_c, ψ_m in $L^2[-1,1]$, and ψ_m in $L^2(-\infty,\infty)$ provides the lemma.

$$\begin{aligned} Q_c(\psi_m)(x+n) &= \frac{1}{\pi}\int_{-1}^{1}\left(\frac{c}{2}\int_{-1}^{1} e^{ic(x+n-t)s}ds\right)\psi_m(t)dt \quad \text{by (7)} \\ &= \frac{c}{2\pi}\int_{-1}^{1} e^{ic(x+n)s}\left(\int_{-1}^{1} e^{-icst}\psi_m(t)dt\right)ds \\ &= \frac{c}{2\pi}\overline{\lambda_m}\int_{-1}^{1} e^{ic(x+n)s}\psi_m(s)ds \quad \text{by (2)} \\ &= \frac{c}{2\pi}\left|\lambda_m\right|^2\psi_m(x+n) \quad \text{by (13).} \end{aligned}$$

2.4. **Band-limited functions.** The Sinc-transformation operator $P_c : L^2(\mathbf{R}) \to L^2(\mathbf{R})$ defined by

$$P_c(\phi) = \frac{1}{\pi}\int_{-\infty}^{\infty}\frac{\sin c(x-t)}{x-t}\phi(t)dt \tag{15}$$

is a projection operator from $L^2(-\infty,\infty)$ onto a subspace of "band-limited" functions which will be defined later in this subsection. The following lemma gives an important starting point toward the projection property of P_c.

Lemma 2.6. *The Sinc-transformation operator P_c becomes the identity operator for the function space spanned by $\psi_m(x)$ in $L^2(-\infty,\infty)$,*

$$P_c(\psi_m)(x) = \frac{1}{\pi}\int_{-\infty}^{\infty} \frac{\sin c(x-t)}{x-t}\psi_m(t)dt = \psi_m(x). \tag{16}$$

Proof.

$$\begin{aligned} P_c(\psi_m)(x) &= \int_{-\infty}^{\infty}\left(\frac{c}{2\pi}\int_{-1}^{1} e^{ic(x-t)s}ds\right)\left(\frac{1}{\lambda_m}\int_{-1}^{1} e^{icty}\psi_m(y)dy\right)dt \quad \text{by (13)} \\ &= \frac{1}{\lambda_m}\int_{-1}^{1}\psi_m(y)\left(\int_{-1}^{1} e^{ixs}\left(\frac{1}{2\pi}\int_{-\infty}^{\infty} e^{ic(y-s)t}d(ct)\right)ds\right)dy \\ &= \frac{1}{\lambda_m}\int_{-1}^{1} e^{icxy}\psi_m(y)dy = \psi_m(x) \quad \text{by (13).} \end{aligned}$$

A function f in $L^2(-\infty,\infty)$ is a band-limited function with band-limit c if $f(x)$ is in the following form,

$$f(x) = \int_{-1}^{1} e^{icxt}\sigma(t)dt \tag{17}$$

for any $\sigma \in L^2[-1,1]$. The following lemma extends Lemma 2.6 to any band-limited function.

Lemma 2.7. *For a band-limited function $f(x) = \int_{-1}^{1} e^{icxy}\sigma(y)dy$, P_c is a projection operator onto itself,*

$$P_c(f)(x) = \frac{1}{\pi}\int_{-\infty}^{\infty} \frac{\sin c(x-t)}{(x-t)}f(t)dt = f(x). \tag{18}$$

Proof.

$$\begin{aligned} P_c(f)(x) &= \int_{-\infty}^{\infty}\left(\frac{c}{2\pi}\int_{-1}^{1} e^{ic(x-t)s}ds\right)\left(\int_{-1}^{1} e^{icty}\sigma(y)dy\right)dt \\ &= \int_{-1}^{1}\left(\int_{-1}^{1} e^{icxs}ds\left(\frac{1}{2\pi}\int_{-\infty}^{\infty} e^{ict(y-s)}d(ct)\right)ds\right)\sigma(y)dy \\ &= \int_{-1}^{1} e^{icxy}\sigma(y)\,dy \;=\; f(x) \end{aligned}$$

P_c is the orthogonal projection operator onto the space of functions of band-limit c on $(-\infty,\infty)$. It is clear that $\{\psi_m(x) = \frac{1}{\lambda_m}\int_{-1}^{1} e^{icxt}\psi_m(t)dt\}$ are band-limited functions and complete in the set of band-limited functions since $\{\psi_m\}$ are complete in $L^2[-1,1]$. Note that $\int_{-\infty}^{\infty}\frac{\sin c(x-u)}{\pi(x-u)}\frac{\sin c(u-s)}{\pi(u-s)}du = \frac{\sin c(x-s)}{\pi(x-s)}$ since $\frac{\sin c(x-s)}{x-s}$ is also a band-limited function. □

Theorem 2.8. *For any band-limited function $f(x)$ with band-limit c, an inner product of $f(x)$ and $\psi_m(x)$ in $L^2(-\infty,\infty)$ can be inferred from that in $L^2[-1,1]$,*

$$\int_{-\infty}^{\infty}\psi_m(x)f(x)dx=\frac{1}{\mu_m}\int_{-1}^{1}\psi_m(x)f(x)dx \tag{19}$$

Proof.

$$\begin{aligned}\int_{-\infty}^{\infty}\psi_m(x)f(x)dx &= \int_{-\infty}^{\infty}\left(\frac{1}{\mu_m}\int_{-1}^{1}\psi_m(t)\frac{\sin c(x-t)}{\pi(x-t)}dt\right)\,f(x)\,dx \quad \text{by (14)}\\ &= \frac{1}{\mu_m}\int_{-1}^{1}\psi_m(t)\left(\int_{-\infty}^{\infty}\frac{\sin c(x-t)}{\pi(x-t)}f(x)dx\right)dt\\ &= \frac{1}{\mu_m}\int_{-1}^{1}\psi_m(t)f(t)dt \quad \text{by (18).}\end{aligned}$$

As a corollary, the orthogonality of the prolate functions $\psi_m(x)$ in $L^2(-\infty,\infty)$,

$$\int_{-\infty}^{\infty}\psi_m(x)\psi_n(x)\,dx=\frac{1}{\mu_m}\delta_{mn} \tag{20}$$

can be proven from the orthonormality of $\{\psi_m(x)\}$ in $L^2[-1,1]$, $\int_{-1}^{1}\psi_m(x)\psi_n(x)dx=\delta_{mn}$.

2.5. **Fourier Integral.** We define the Fourier transform on the set of compactly-supported complex-valued functions of R and extend to $L^2(R)$. Then $F:L^2(-\infty,\infty)\to L^2(-\infty,\infty)$ and $F^*:L^2(-\infty,\infty)\to L^2(-\infty,\infty)$ defined as

$$H(k) := F(h)(k) = \frac{1}{\sqrt{2\pi}}\int_{-\infty}^{\infty}e^{-ikx}h(x)\,dx \tag{21}$$

$$h(x) := F^*(H)(x) = \frac{1}{\sqrt{2\pi}}\int_{-\infty}^{\infty}e^{ikx}H(k)\,dk \tag{22}$$

are unitary operators. That is, $F^*=F^{-1}$.

The function spaces in $L^2(-\infty,\infty)$ spanned by the truncated prolate functions

$$\Psi_m(cx):=\begin{cases}\frac{1}{\sqrt{2\pi}}\frac{\lambda_m}{\mu_m}\psi_m(x) & \text{if } |x|<1,\\ 0 & \text{if } |x|>1,\end{cases} \tag{23}$$

and by prolate functions $\{\psi_m(k)\}$ are dual under the Fourier transformation in $L^2(-\infty,\infty)$.

Theorem 2.9. *Suppose that c is real and positive. For $x,k\in(-\infty,\infty)$,*

$$F(\Psi_m)(k)=\psi_m(k) \;\; \textit{and} \;\; F^*(\psi_m)(cx)=\Psi_m(cx) \tag{24}$$

Proof.

$$\begin{aligned}
F(\Psi_m)(k) &= \frac{1}{\sqrt{2\pi}}\int_{-\infty}^{\infty} e^{-ik(cx)}\Psi_m(cx)\, d(cx) \\
&= \frac{c}{2\pi}\frac{\lambda_m}{\mu_m}\int_{-1}^{1} e^{-ickx}\psi_m(x)\, dx \;=\; \psi_m(k) \quad \left(\because \frac{c}{2\pi}\frac{\lambda_m\overline{\lambda_m}}{\mu_m} = 1\right) \\
F^*(\psi_m)(cx) &= \frac{1}{\sqrt{2\pi}}\int_{-\infty}^{\infty} e^{ik(cx)}\frac{1}{\overline{\lambda_m}}\left(\int_{-1}^{1} e^{-icks}\psi_m(s)ds\right) dk \quad \text{by (13)} \\
&= \frac{1}{\sqrt{2\pi}}\frac{1}{\overline{\lambda_m}}\int_{-1}^{1}\frac{2\pi}{c}\delta(x-s)\psi_m(s)\, ds \quad \left(\because \frac{c}{2\pi}\int_{-\infty}^{\infty} e^{icks}dk = \delta(s)\right) \\
&= \begin{cases} \frac{1}{\sqrt{2\pi}}\frac{\lambda_m}{\mu_m}\psi_m(x)\,, & \text{if } |x|<1 \\ 0\,, & \text{if } |x|>1 \end{cases}.
\end{aligned}$$

3. PROLATE FUNCTION BASED INVERSION METHODS

Suppose we have Fourier coefficients $\{s_n\}_{n=1}^N$ of an object of finite size $f(x)$ at finite number of measurement points $\{k_n : |k_n| < K\}_{n=1}^N$ in frequency space,

$$s_n = \int_{-\infty}^{\infty} e^{-ik_n x} f(x)dx \tag{25}$$

where

$$f \;\in\; L^2(X) := \{f \in L^2(\mathbf{R}) \;:\; f(x) = 0,\; |x| > X\}. \tag{26}$$

We can represent any function $f(x)$ in $L^2(X)$ using prolate coefficients $\{f_m\}_{m=0}^{\infty}$,

$$f(x) = \sum_{m=0}^{\infty} f_m \psi_m^c\left(\frac{x}{X}\right) \tag{27}$$

since the function space spanned by the prolate functions with $c = XK$ is complete in $L^2(X)$. It is sometimes convenient to define a Fourier transformation matrix $\mathbf{F}$ which maps the prolate coefficient vector $\mathbf{f} = \{f_m\}_{m=0}^{\infty}$ to the corresponding Fourier signal vector $\{Ff\,(k_n)\}_{n=1}^N$,

$$\mathbf{F}\,\mathbf{f} \;=\; \mathbf{F}\begin{pmatrix} f_0 \\ f_1 \\ \vdots \end{pmatrix} \;=\; \begin{pmatrix} Ff\,(k_1) \\ \vdots \\ Ff\,(k_N) \end{pmatrix}. \tag{28}$$

Our goal in this section is to find a minimum norm solution $g(x)$ in $L^2(X)$ or the prolate coefficient vector $\mathbf{g}$ whose Fourier signal $Fg(k_n)$ matches with the measurement data $\mathbf{s} = \{s_n\}_{n=1}^N$ with maximum error bound ϵ,

$$\min_{g\in L^2(X)} ||g(x)||_{L^2(X)} \quad \text{subject to} \quad ||Fg\,(k_n) - s_n||_{l_2}^2 \le \epsilon^2. \tag{29}$$

In some cases, it is preferable to obtain a minimum norm solution using a norm other than $L^2(X)$ norm. So we can slightly generalize the previous task (29) to the following constraint optimization problem whose object is minimizing $||Qg(x)||_{L^2(X)}$ instead of $||g(x)||_{L^2(X)}$,

$$\min_{g\in L^2(X)} ||Qg(x)||_{L^2(X)} \quad \text{subject to} \quad ||Fg\,(k_n) - s_n||_{l_2}^2 \leq \epsilon^2 \tag{30}$$

where Q is a unitary operator from $L^2(X)$ onto itself whose null space is a subset of the null space of F, $Null(Q) \subset Null(F)$. Let $\mathbf{Q}$ denote the discrete version of Q with prolate basis functions.

3.1. **Interpolation based inversion Method.** Suppose we want to find an optimal solution $\mathbf{g} \in L^2(X)$ of (30) with a given signal $\mathbf{s}$ in terms of prolate coefficients,

$$\min ||\mathbf{Q}\,\mathbf{g}|| \quad \text{subject to} \quad ||\mathbf{F}\,\mathbf{g} - \mathbf{s}|| = \epsilon \tag{31}$$

where $\mathbf{g}(x) = \sum_m \mathbf{g}_m \psi_m(x)$, $s(k_n) = \sum_m \mathbf{d}_m \psi_m(k_n)$, $(\mathbf{Fg})_n = \sum_m \chi_m \mathbf{g}_m \psi_m(k_n)$, and an image quality measurement operator Q is a diagonal operator, $Q\ \psi_m(x) = q_m \psi_m(x)$ for $|x| < X$. We define a Lagrangian minimizer function $\Phi(g)$ with a Lagrange multiplier λ^{-2},

$$\Phi(g) := ||Qg(x)||_{L^2(X)}^2 + \lambda^{-2}\left(||Fg\,(k_n) - s_n||^2 - \epsilon^2\right). \tag{32}$$

We take the partial derivatives with respect to g_i in order to solve the constrained minimization (30), which implies the following identity

$$\mathbf{g}_m = \frac{\overline{\chi_m}}{\overline{\chi_m}\chi_m + \lambda^2 \overline{q_m} q_m}\mathbf{d}_m. \tag{33}$$

Once λ is given, $\mathbf{g}(\lambda)$ can be explicitly computable from the given prolate coefficients $\mathbf{d}$ of the signal, and a proper Lagrangian multiplier λ can be found from the constraint equation $||\mathbf{F}\,\mathbf{g}(\lambda) - \mathbf{s}|| = \epsilon$.

3.2. **Lagrangian Multiplier Method.** We define a Lagrangian minimizer function $\Phi(g)$ with a Lagrange multiplier λ and a slack variable μ,

$$\Phi(g) := ||Qg(x)||_{L^2(X)}^2 + \lambda\left(||Fg\,(k_n) - s_n||^2 + \mu^2 - \epsilon^2\right) \tag{34}$$

and take the partial derivatives with respect to λ, μ, and g_i in order to solve the constrained minimization (30),

$$\frac{\partial \Phi}{\partial \lambda} = ||\mathbf{Fg} - \mathbf{s}||^2 + \mu^2 - \epsilon^2\,, \tag{35}$$

$$\frac{\partial \Phi}{\partial \mu} = 2\lambda\mu\,, \tag{36}$$

$$\frac{\partial \Phi}{\partial g_i} = 2\lambda(\mathbf{Fg} - \mathbf{s}, \mathbf{F}e_i) + 2(\mathbf{Qg}, \mathbf{Q}e_i) \tag{37}$$

where e_i is the i-th unit vector and $(\cdot,\cdot)$ denotes the vector inner product.

There are two cases to make all derivatives to zero. The first trivial case comes with $\lambda = 0$, $(\mathbf{Qg}, \mathbf{Q}e_i) = 0$ which implies $||Qg(x)||_{L^2(X)} = 0$ or $g(x) \in Null(Q) \subset Null(F)$. We ignore

this case since it is meaningless to distinguish the solution from the zero solution if the norm of the measured data $\mathbf{s}$ is smaller than the measurement error bound ϵ, $||s_n||^2 + \mu^2 = \epsilon^2$. The second case comes with $\mu = 0$ and $g(x)$ satisfies

$$||\mathbf{F}\,\mathbf{g} - \mathbf{s}||^2 \;=\; \epsilon^2\,, \tag{38}$$

$$\left(\mathbf{F}^*\mathbf{F} + \frac{1}{\lambda}\mathbf{Q}^*\mathbf{Q}\right)\mathbf{g} \;=\; \mathbf{F}^*\mathbf{s}. \tag{39}$$

For any given $\lambda > 0$, $\left(\mathbf{F}^*\mathbf{F} + \frac{1}{\lambda}\mathbf{Q}^*\mathbf{Q}\right) : Null(\mathbf{Q})^\perp \to Range(\mathbf{Q}^*)$ is a strictly positive operator and the second equation (39) with a right-hand-side $\mathbf{F}^*\mathbf{s}$ in the range of the operator can be solved uniquely in a solution space $Null(\mathbf{Q})^\perp = \overline{Range(\mathbf{Q}^*)}$, which guarantees the uniqueness of $\mathbf{F}\mathbf{g}_\lambda$. The solution $\mathbf{g}_\lambda$ is then used to solve the one variable equation (38) a with respect to λ, which is usually solved iteratively.

3.3. **Minimum norm solution in $L(X)$.** We restrict ourself to the $L(X)$ minimization problem (29) or (30) with $Q = I$,

$$\min_{g\in L^2(X)} ||g(x)||_{L^2(X)} \quad \text{subject to} \quad ||Fg\,(k_n) - s_n||_{l_2}^2 \le \epsilon^2. \tag{40}$$

Then a nontrivial solution $g(x)$ satisfies $\left(\mathbf{F}^*\mathbf{F} + \frac{1}{\lambda}I\right)\mathbf{g} \;=\; \mathbf{F}^*\mathbf{s}$ and $||\mathbf{F}\mathbf{g} - \mathbf{s}||^2 \;=\; \epsilon^2$ for some $\lambda > 0$. For a given λ, the first equation has a unique solution $\mathbf{g}_\lambda$ in $Range(\mathbf{F}^*)$, thus it can be written as following form, $\mathbf{g}_\lambda \;=\; \mathbf{F}^*\,\mathbf{z}_\lambda$. The equation multiplied by $\mathbf{F}$ becomes $\left(\mathbf{F}\mathbf{F}^*\mathbf{F}\mathbf{F}^* + \frac{1}{\lambda}\mathbf{F}\mathbf{F}^*\right)\mathbf{z}_\lambda = \mathbf{F}\mathbf{F}^*\,\mathbf{s}$, whose solutions are unique up to the difference in the null space of $\mathbf{F}^*$. The following system of equations for λ and $\mathbf{g}_\lambda$

$$\left(\mathbf{M} + \frac{1}{\lambda}\mathbf{I}\right)\mathbf{z}_\lambda \;=\; \mathbf{s} \tag{41}$$

$$||\mathbf{M}\,\mathbf{z}_\lambda - \mathbf{s}||^2 \;=\; \epsilon^2 \tag{42}$$

provides a unique solution even for a rank-deficient operator $\mathbf{M} = \mathbf{F}\mathbf{F}^*$ and $\mathbf{g}_\lambda = \mathbf{F}^*\,\mathbf{z}_\lambda$ is the solution of the minimization problem (40).

4. NUMERICAL EXAMPLES AND CONCLUSION

We have implemented two numerical schemes presented in section 3.1 and 3.2–3.3 using MATLAB. The solid line in Figure 3 and 4 shows our numerical test function in $L^2([-\frac{1}{2}, \frac{1}{2}])$ which includes one exponential and two box functions. The corresponding Fourier coefficient function has been computed analytically and signal data $\mathbf{s}_n$ have been sampled at 128 points in frequency space $|k| \le 32$. We use the prolate spheroidal wave functions of order zero with $c = 32\pi$ whose eigenvalues are $|\lambda_m| \approx 0.25, m \le 64$, $|\lambda_{76}| \approx 10^{-5}$, and $|\lambda_{87}| \approx 10^{-10}$.

Example 1 (Interpolation Based Inversion) In this example, we compute up to 80 prolate coefficients $\mathbf{d}_m$ from the given Fourier signal $Fg(k_n)$, $k_{p+64} = sign(p)\,\frac{32\,p^2}{64^2},\ p = -63, \cdots, 64$. Once a smoothing parameter $\lambda^2 q_m$ is given, evaluation of $g(x) \in L^2([-\frac{1}{2}, \frac{1}{2}])$ from the interpolation coefficients $\mathbf{d}_m$ with aid of the formula (33) is a trivial job.

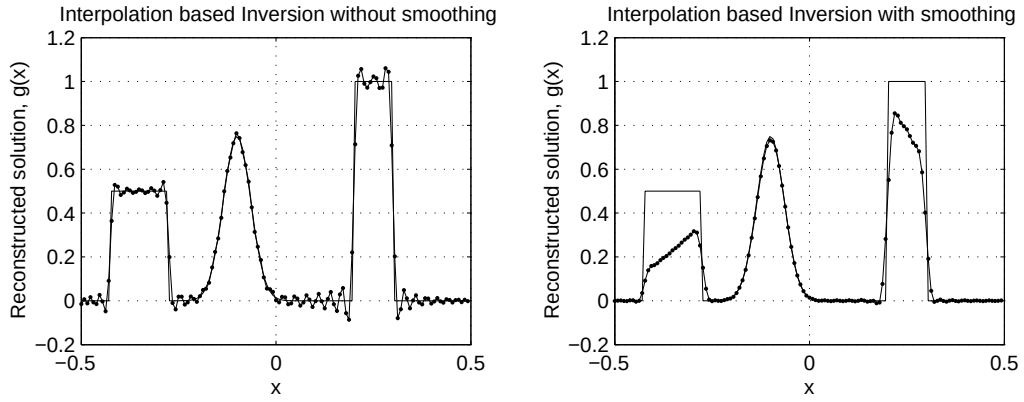

FIGURE 3. Results of Interpolation based inversion.

Figure 3 shows two results with different smoothing parameters. The left plot shows a result with almost no smoothing effect where we set $\lambda^2 q_m \approx 10^{-8}$ while the right plot is done with $\lambda^2 q_m \approx 10^{-4} m^2$. The result in the right plot is a somewhat extreme case in the sense that we put too much smoothing effect and the heights of box function are significantly reduced from the original heights. It is also worth to notice that the exponential function has been less damaged even with such an extreme smoothing parameters. We did not make an effort to find a best smoothing parameters, which is, of course, an essential task in real applications.

Example 2 (Lagrangian Multiplier Based Inversion) In this example, we compute an optimal solution $g(x) \in L^2(X)$ using the Lagrangian optimization technique presented in section 3.2–3.3.

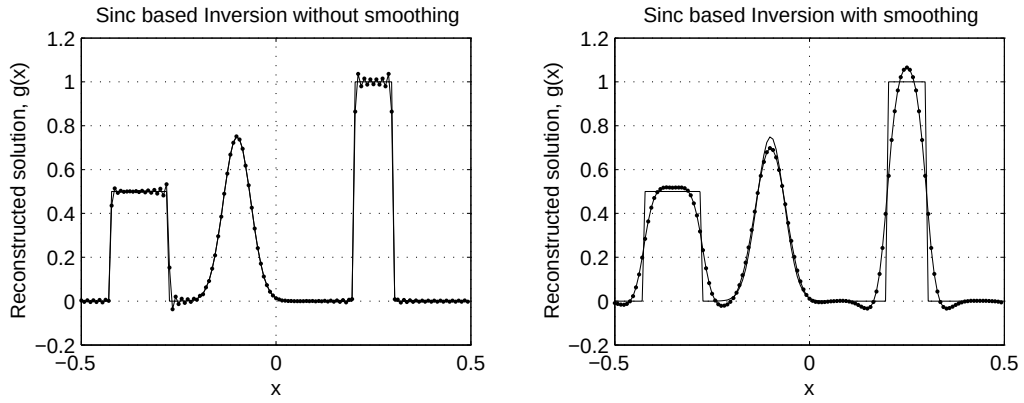

FIGURE 4. Results of Lagrangian Multiplier based inversion.

Figure 4 shows two results with different smoothing parameters. The left result comes with $\frac{1}{\lambda} = 10^{-10}$ and the right with a diagonal operator $\mathbf{Q}_{nn} = n^2$ and $\frac{1}{\lambda} = 10^{-4}$. Again, these two extreme cases are just for demonstration and we may find much better tuning parameters λ and $\mathbf{Q}$ depending on the real situation.

The computation cost of the Sinc-operator based inversion is little bit more expensive than the interpolation based one because the linear system (41) must be solved for each choice of Lagrangian multiplier. However, it is numerically much stabler than the interpolation based algorithm when data sampling points k_n is badly placed. Our implementations and numerical simulations given in this section are rather primitive to use real applications, however, it clearly shows feasibility of the algorithms for signal processing applications.

REFERENCES

[1] F. Gantmacher and M. Krein, *Oscillation Matrices and Kernels and Small Oscillations of Mechanical Systems*, Revised edition. AMS Chelsea Publishing, Providence, RI, 2002.

[2] K. Khare, *Sampling theorem, band-limited integral kernels and inverse problems*, Inverse Problems 23 (2007) 1395–1416.

[3] K. Khare and N. George, *Sampling theory approach to prolate spheroidal wavefunctions*, J. Phys. A: Math. Gen. 36 (2003) 10011–10021.

[4] S. Kunis and D. Potts, *Stability results for scattered data interpolation by trigonometric polynomials*, SIAM J. Sci. Comput. 29 (2007) 1403–1419.

[5] H.J. Landau and H. Widom, *Eigenvlue distribution of time frequency limiting*, J. Math. Anal. Appl., 77 (1980) 469–481.

[6] D. Slepianand, *Some asymptotic expansions for prolate spheroidal wave functions*, J. Math. Phys., 44 (1965) 99–140.

[7] D. Slepian and H. Pollak, *Prolate spheroidal wave functions, Fourier analysis and uncertainty. I. and II.*, Bell System Tech. J., 40 (1961) 43–63 and 65–84.

[8] D. Slepian and H. Pollak, *Prolate spheroidal wave functions, Fourier analysis and uncertainty. III. The Dimension of the Space of Essentially Time- and Band-Limited Signals*, Bell System Tech. J., 41 (1962) 1295–1336.

[9] D. Slepian, *Prolate spheroidal wave functions, Fourier analysis and uncertainity. IV. Extensions to many dimensions; generalized prolate spheroidal functions*, Bell System Tech. J., 43 (1964) 3009–3057.

[10] D. Slepian, *Prolate spheroidal wave functions, Fourier analysis and uncertainity. V. Discrete Case*, Bell System Tech. J., 57 (1978) May–June.

[11] J. Stratton, P. Morse, L. Chu, J. Little, and F. Corbató, *Spheroidal wave functions*, the technology press of M.I.T., 1956.

[12] H. Xiao, V. Rokhlin, and N. Yarvin, *Prolate shperioical wavefunctions, quadrature and interpolation*, Inverse Prob., 17 (2001) 805–838.

[13] H. Xiao and V. Rokhlin, *High-Frequency Asymptotic Expansions for Certain Prolate shperioical wavefunctions*, J. Fourier Anal. and Appl., 9 (2003) 575–596.